Compound Bar Assembly Primer

Sriharsha Sheshanarayana (ssheshanarayana01@qub.ac.uk), Prof Cecil Armstrong (c.armstrong@qub.ac.uk), and Prof Adrian Murphy (a.murphy@qub.ac.uk)

School of Mechanical and Aerospace Engineering,
Queen's University Belfast, Belfast UK
16/03/2021

1.1 Introduction

The primary motivation behind this primer is to introduce the reader to the concepts of *characteristic loads* and *performance envelopes* using an insightful yet straightforward problem of a compound bar assembly.

Though the previous works by McGuinness and Dharmasaroja [1, 2] have examined characteristic loads and performance envelopes using a real-world aircraft level example, there are many advantages of using the compound bar assembly example. The rationale for choosing it is -

- The assembly problem being simple provides a strong intuitive understanding of the concepts.
- Complete control over the entire process - from loads generation to structural and geometric definitions.
- The performance envelope of the assembly problem is represented in 2-dimensional space which is better for visualisation.
- Structural constraints have analytical equations as opposed to many black-box solutions typically found with the aircraft level example.
- Additional study of pre-stressed structure is carried out which includes additional load types such as thermal or gravitational loads. The simple assembly enables the behaviour and benefits of characteristic loads and performance envelopes to be studied under these loads.

Efforts have been made throughout the chapter to draw parallels between a generic aircraft design process and the compound bar assembly problem. The terminologies introduced in this

chapter are used in the aircraft level examples later in the thesis as well. The remainder of this thesis will use the assembly example initially when new concepts are introduced. It is then followed by a more realistic model - such as a stiffened panel of an aircraft wing top cover. The reader is encouraged to refer to this example problem.

1.2 Compound Bar Assembly

The compound bar assembly consists of two elements, a hollow tube, and a solid bar, as shown in Figure 0.1. The tube and the bar are made up of Aluminium 6061-O [3] and ASTM A36 Steel [4] respectively. The assembly is clamped at the bottom, and the free end is constrained such that both the bar and the tube have equal longitudinal deformations (strains) upon loading. The assembly follows the assumptions of the Euler-Bernoulli beam, i.e. a cross-sectional plane in the assembly will remain plane during deformation, see textbook by Benham *et al.* [5] for further reading. An axial force F and a bending moment M is applied at the neutral axis.

Later, thermal loads are introduced as a change in the temperature from the assembly temperature. This situation replicates a more generic case of non-zero loading conditions (e.g. loading due to residual stress from manufacturing and stationary gravity loads) often seen within aircraft design.

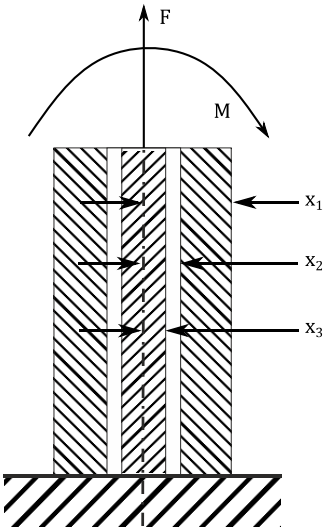

Figure 0.1: Compound bar assembly.

Table 0.1 gives the dimensions of the compound bar assembly along with other material properties of both the elements. Terms σ_t^{ten} and σ_t^{comp} are the yield stress of the tube in tension

and compression, respectively. σ_b^{ten} and σ_b^{comp} are the yield stress of the bar in tension and compression, respectively. Terms E_t and E_b are the Young's modulus of tube and bar and α_t and α_b are the thermal coefficients.

Attribute	Value	Units
x1	0.2	m
x2	0.18	m
x3	0.11	m
σ_t^{ten}	55.2	MPa
σ_t^{comp}	103	MPa
E_t	70	GPa
σ_b^{tens}	250	MPa
σ_b^{comp}	152	MPa
E_b	230	GPa
α_t	24e-6	/C
α_b	12e-6	/C

Table 0.1: Properties of the compound bar assembly

1.3 Load case

In aircraft design, a single load case is composed of various instances of loads (such as shear, torque or bending moment etc.) acting on the structure. The structure is then sized using a static analysis approach. A dynamic case such as an aircraft making a turn (manoeuvring loads) is analysed as a pseudo-static load by discretising the continuous loads acting on the structure into small time intervals and treating each time instance as a separate load case. This approach is a standard industry practice.

Along with the textbook load cases directed by the certification body, the flight loads from the manoeuvring and the gust cases can result in hundreds or thousands of load cases for which the

aircraft structure must be assessed. Therefore, the compound bar assembly is analysed for one such dynamic load scenario.

To simulate a dynamic case for the compound bar assembly, a pair of spring-mass-damper systems are used, as shown in Figure 0.2. With an initial velocity on the mass, the spring-mass-damper system will impart a reaction force which is then transferred to the assembly.

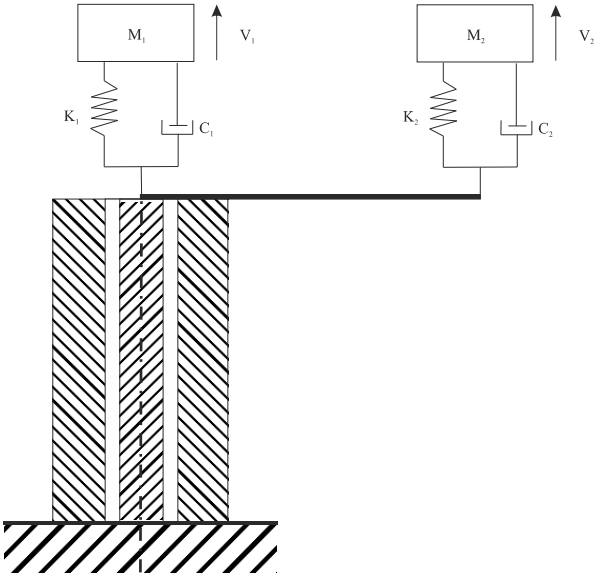

Figure 0.2: Compound bar assembly with the pair of spring-mass-damper systems generating the required forces.

The first spring-mass-damper system is attached directly to the compound bar assembly at the neutral axis. This will impart the axial loading resulting in tension and compression within the assembly. The second spring-mass-damper system is attached to an arm having infinite stiffness, creating the necessary bending moment on the assembly. Since the assembly respects the Euler-Bernoulli beam, the cross-sectional plane remains in the same plane, and therefore, the top plane of the assembly remains and deforms as a plane.

This two-system loading is considered to make sure that the bending moment and axial force are truly decoupled, i.e. independent of each other. Such an approach makes the loads on the assembly problem more interesting for the study.

The axial force and bending moments generated from the spring-mass-damper system are thus referred to as *external loads* from here on in this document. For the aircraft problem, the

external loads will correspond to the aerodynamic pressure distribution, inertia forces due to the mass, etc. and are usually passed in the SMT format.

The time-series history of external loads generated by the pair of spring-mass-damper system for a combination of velocity and mass is given in Figure 0.3. These results were generated by solving an ordinary differential equation (ODE) of a spring-mass-damper system given in Eq. 0.1. The Python *odeint* Scipy [6] implementation is used to solve the ODE

$$M\frac{d^2x}{dt^2} + C\frac{dx}{dt} + Kx = 0 \qquad (0.1)$$

where M is the mass, C is the damping coefficient, K is the stiffness and x is the displacement. The damping coefficient is calculated as $C = \xi C_c$, C_c is the critical damping of the system given by $C_c = 2\sqrt{K\mathrm{M}}$. The mass and velocity initial conditions are given in Table 0.2[1].

Property	Value	Units
M_1	1e5	kg
V_1	120	m/s
K_1	5e3	N/m
ξ_1	0.3	
M_2	1e5	kg
V_2	110	m/s
K_2	9e3	N/m
ξ_2	0.5	
arm	0.3	m

Table 0.2: Properties used in the dynamic model, ξ is the damping ratio

By considering m time intervals, the external forces can be arranged in a matrix form. A row of the matrix represents each time step, and the column represents the axial force and the

[1] The large magnitudes of the mass and velocities are physically impractically in the real world. However, these values provide a good visualisation of the envelope.

bending moment as given in Eq. 0.2. Therefore, matrix P which represents these external loads is termed as the *external load matrix* and is of the size $m \times 2$ for the assembly problem.

$$P = \begin{bmatrix} F_1 & M_1 \\ F_2 & M_2 \\ & \vdots \\ F_m & M_m \end{bmatrix} \tag{0.2}$$

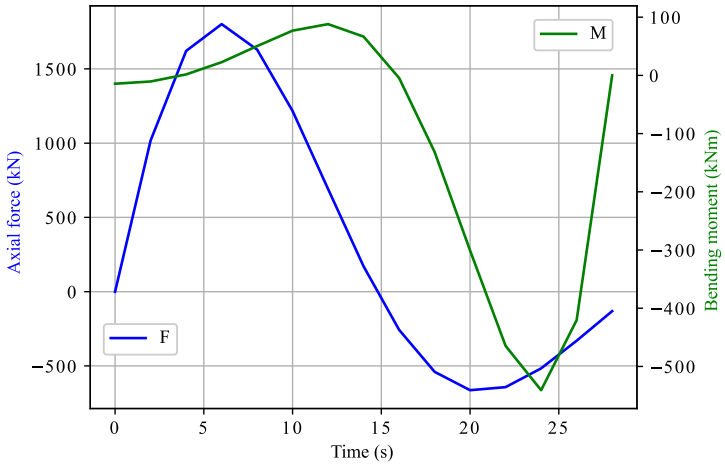

Figure 0.3: External loads time history, axial force and bending moment generated by the pair of spring-mass-damper system

Each external load case will result in *internal loads* inside the elements of the assembly. These internal loads represent how the external loads are distributed within the system (*load paths*). The load paths within the compound bar assembly are computed by solving the equation of the system as given in Eq. 0.3. For example, the axial force on the structure will generate an internal axial force in the tube element and an internal axial force in the bar element. The matrix Γ gives the load path distribution, as shown in Eq. 0.4. Appendix A provides a detailed explanation of calculating Γ matrix.

$$N = P\,\Gamma \tag{0.3}$$

$$\Gamma = \begin{bmatrix} \dfrac{E_t A_t}{(E_t A_t + E_b A_b)} & 0 & \dfrac{E_B A_b}{(E_t A_t + E_b A_b)} & 0 \\ 0 & \dfrac{E_t I_t}{E_t I_t + E_b I_b} & 0 & \dfrac{E_b I_b}{E_t I_t + E_b I_b} \end{bmatrix} \tag{0.4}$$

All the internal loads of the compound bar assembly problem can be represented as a matrix N, termed as the *internal load matrix.* The internal load matrix N has the rows corresponding to the number of load cases and the columns correspond to the different loads as shown by Eq. 0.5.

$$N = \begin{bmatrix} f_1^t & m_1^t & f_1^b & m_1^b \\ f_2^t & m_2^t & f_2^b & m_2^b \\ & & \vdots & \\ f_m^t & m_m^t & f_m^b & m_m^b \end{bmatrix} \tag{0.5}$$

The terms f and m correspond to the internal axial force and the internal bending moment, respectively. The superscripts t and b correspond to tube and bar. Subscripts correspond to the load case number. Figure 0.4 gives the time series history of the internal loads generated for the external load matrix.

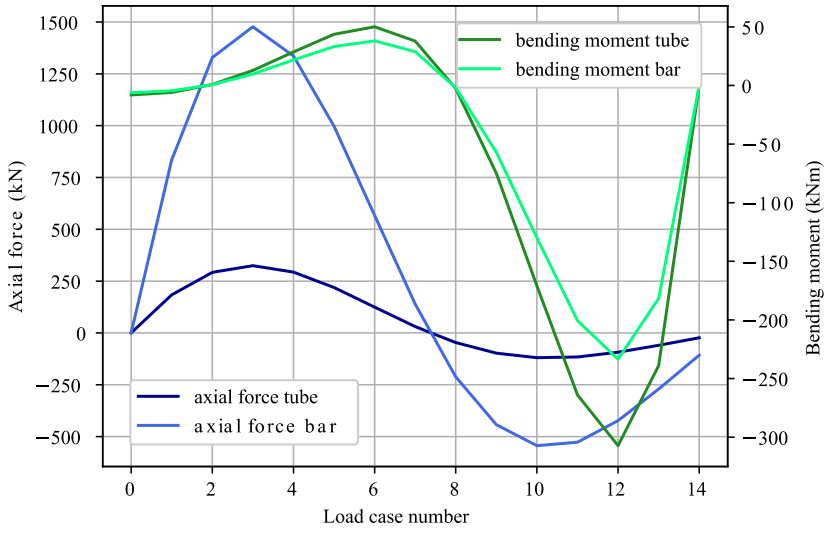

Figure 0.4: Internal loads in the compound bar assembly, produced for a set of 15 external loads

1.4 Characteristic loads decomposition

The characteristic loads are defined as a set of k load cases that when linearly superimposed can reconstruct a large number of load cases with sufficient accuracy. There are many ways to identify such a set of characteristic loads, such as Eigenmodes or interpolation functions. Each

has its own unique advantages and disadvantages when used in the context of the aircraft design process.

With the availability of the loads data, the characteristic loads based on the SVD decomposition will result in identifying the patterns (if it exists within the loads data) and this approach is the most accurate and straightforward. Here, the SVD is implemented to compute the characteristic loads.

1.4.1 Singular value decomposition

The Singular Value Decomposition (SVD) is a popular matrix factorisation technique that is used in many different areas including inverting a matrix (pseudo inverse, least square approximation) and image compressions. SVD decomposes a rectangular matrix A into three component factor matrices as U, Σ and V^* as shown in Eq. 0.6

$$A_{m\times n} = U_{m\times n}\,\Sigma_{n\times n}\,V^*_{n\times n} \tag{0.6}$$

The U and V^* matrices represent the row and the column space. The $*$ represents conjugate transpose. Since the elements of the load matrix do not contain any complex terms, the conjugate transpose is represented by the matrix transpose. The Σ is a non-negative diagonal matrix with diagonal entries arranged in the order of their magnitude $\sigma_1 \geq \sigma_2 \geq \cdots \geq \sigma_n \geq 0$. A detailed explanation of SVD can be found in any linear algebra textbook. However, Appendix **Error! Reference source not found.** gives a graphical interpretation of the SVD factorisation and presents an approach to compute the factored matrices.

Choosing the first k dominant singular values, the Eq. 0.6 can be partitioned as Eq. 0.7, where $\Sigma_{k\times k}$ is first k terms in the diagonal matrix Σ and $r = n - k$ is the rest of the terms.

$$A_{m\times n} = \begin{bmatrix} U_{m\times k} & U_{m\times r} \end{bmatrix} \begin{bmatrix} \Sigma_{k\times k} & 0 \\ 0 & \Sigma_{r\times r} \end{bmatrix} \begin{bmatrix} V^T_{k\times n} \\ V^T_{r\times n} \end{bmatrix} \tag{0.7}$$

The last r terms of the diagonal matrix are relatively small compared to the first k terms; then these values can be rejected. The approximate matrix calculated from rejecting the r terms is shown in Eq. 0.8.

$$A_k = U_{m\times k}\Sigma_{k\times k}\,V^T_{k\times k} \approx A_{m\times n} \tag{0.8}$$

The above form is the reduced rank approximation of the original matrix A and can be called as reduced SVD. A discussion of deriving the SVD factor matrices and the reduced rank approximation is provided in Appendix **Error! Reference source not found.**.

1.4.2 Defining characteristic loads

The product of factor matrices ΣV^T is defined as the characteristic loads matrix $L_{m\times n}$. Eq. 0.9 gives the product of ΣV^T partitioned along k and r terms.

$$L_{m\times n} = \begin{bmatrix} \Sigma_{k\times k} & 0 \\ 0 & \Sigma_{r\times r} \end{bmatrix} \begin{bmatrix} V^T_{k\times n} \\ V^T_{r\times n} \end{bmatrix} \tag{0.9}$$

If the reduced rank approximate matrix is identified for the above equation by rejecting the r terms, then the reduced characteristic load matrix L_k is defined as Eq. 0.10.

$$L_k = \Sigma_{k\times k} V^T_{k\times n} \tag{0.10}$$

The characteristic load matrix L_k will have the same number of columns as the original load matrix. However, the number of rows (corresponding to the number of load cases) is reduced. With the size of the characteristic matrix being $(k \times n)$, the original matrix of size $(m \times n)$ has been reduced from m load cases to k characteristic loads.

$$A_k = U_k L_k \approx A \tag{0.11}$$

1.4.3 Error measurement

The accuracy of the reconstructed matrix A_k can be measured using the Frobenius norm of the matrix as given in the Eq. 0.13. The Frobenius norm is defined as the square root of the sum of all the absolute squares of elements in a matrix A of size $(m \times n)$, as given in Eq. 0.12.

$$\|A\|_F = \sqrt{\sum_{i=1}^{m}\sum_{j=1}^{n}\left|a_{ij}\right|^2} \tag{0.12}$$

The Frobenius norm error is used to decide the number of characteristic loads, k, required to approximate the set of load cases. A detailed discussion on using the Frobenius norm error to

quantify the errors in the characteristic load matrix can be found in the paper by Dharmasaroja *et al.* [7]

$$\varepsilon = \frac{\|A - A_k\|_F \times 100}{\|A\|_F} \tag{0.13}$$

1.4.4 External characteristic loads

The external load matrix P of the compound bar assembly is created by taking 15 samples from the loads time history shown in Figure 0.3. Therefore the external loads matrix composed of axial force and bending moment is of size 15×2. The external load matrix is decomposed using SVD to identify the external characteristic load matrix as Eq. 0.14. The subscript (P) is used to denote that this belongs to the external loads and not to be confused with the internal loads defined in the next section.

$$\begin{aligned} SVD(P) &= U_{(P)}\Sigma_{(P)}V_{(P)}^T \\ P_k &= U_{(P)_k}L_{(P)_k} \approx P \end{aligned} \tag{0.14}$$

Since the assembly problem is simple, the singular value matrix $\Sigma_{(P)}(2 \times 2)$ contains only two singular values in the diagonal. Even without further rank reduction, the number of characteristic loads $L_{(P)_k}$ needed to reconstruct the external loads accurately is identified. The number of characteristic loads identified is equal to two (since there are two independent values of momentum M_1V_1 and M_2V_2 applied to the system).

To aid the reader to interpret these matrices, a numerical calculation for a single load case from the external load case matrix P is presented. The two characteristic loads computed using Eq. 0.14 for the particular load case set are $L_{(P)_k} = \begin{bmatrix} -3021.290\ kN & -751.855\ kNm \\ -2006.862\ kN & 499.412\ kNm \end{bmatrix}$. Considering the fourth row of P corresponding to the fourth load case $P_{LC4} = [1801.76\ kN \quad 22.6\ kNm]$. The corresponding characteristic coefficient is $U_{(P_{LC4})_k} = [-0.3132 \quad -0.4262]$. The dot product of the characteristic coefficient with the characteristic loads yields $P_{k_{LC4}}$ which is approximately to P (subject to rounding off error) in this example as given in Eq. 0.15.

$$P_{k_{LC4}} = U_{(P_{LC4})_k}L_{(P)_k} = [1801.59\ kN \quad 22.63\ kNm] \approx P_{LC4} \tag{0.15}$$

A similar reconstruction of the external loads using characteristic loads is performed for all the load cases. The reconstructed external load P_k is compared with the actual external load case matrix P, as shown in Figure 0.5. Since the Frobenius norm error between P_k and P is zero, reconstruction is exact.

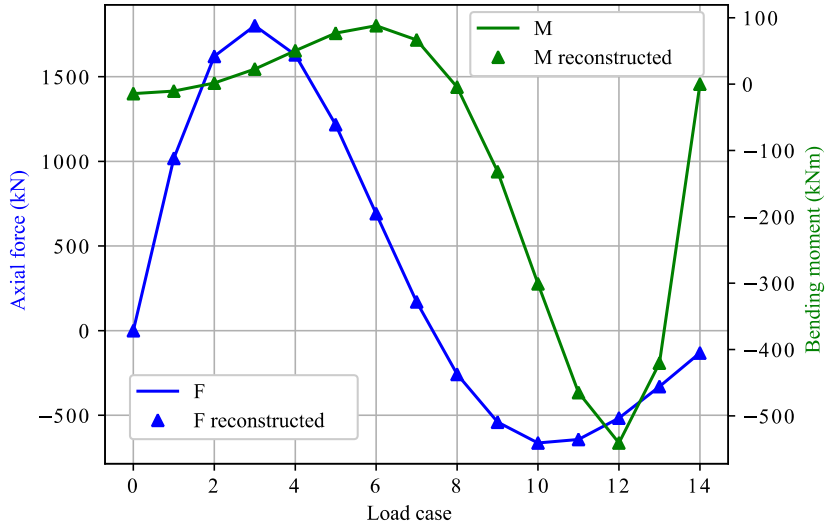

Figure 0.5: External load time history vs reconstructed loads from external characteristic load matrix. Reconstructed loads given by dashed lines

Note that if both the axial force and bending moment were to be generated by using a single spring-mass-damper system at the end of the moment arm, then just one characteristic load would have been enough to reconstruct all the load cases. This is because the bending moment will be a linear multiple (equal to the arm) of the force from the spring-mass-damper system.

1.4.5 Internal characteristic loads

The internal load case matrix $N(15 \times 4)$ is computed for the 15 external load cases from Eq. 0.16. The internal load matrix can also be decomposed using SVD to identify the set of *internal characteristic loads*, as shown in Eq. 0.16. The subscript (N) indicates that the characteristic loads are for the internal load case set. Therefore, ${U_{(N)}}_k$ and ${L_{(N)}}_k$ are the characteristic coefficient and characteristic load for the internal load matrix N respectively.

$$SVD(N) = U_{(N)}\Sigma_{(N)}V_{(N)}^T$$
$$N_k = {U_{(N)}}_k {L_{(N)}}_k \approx N \tag{0.16}$$

The initial number of singular values identified by $\Sigma_{(N)}$ is equal to four, but the last two singular values are close to zero and thus can be rejected without a large loss in accuracy. The Frobenius norm error for the reduced rank, $k = 2$ is zero. A comparison of this error using different ranks are presented in Figure 0.6.

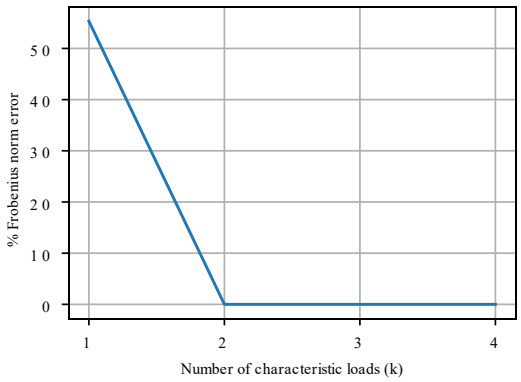

Figure 0.6: Frobenius norm error vs the number of characteristic loads (k), for the assembly internal loads

Using these internal characteristic loads $L_{(N)_k}$, the complete internal load matrix N is reconstructed, as shown in Figure 0.7.

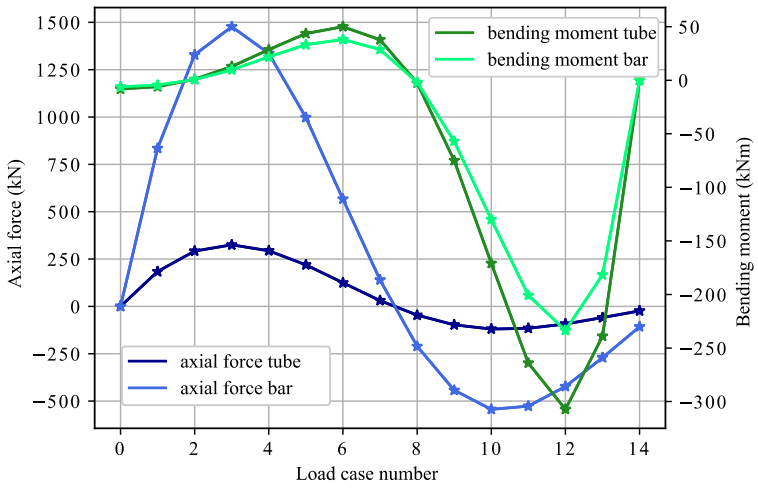

Figure 0.7: Internal loads in the assembly (lines) and reconstructed loads represented by the star (*), for k = 2

An intuitive way to interpret this result is by looking at the relation between the 2 types of external load (columns of P) and 4 types of internal loads (columns of N) internal loads. For

example, an axial force will generate an internal load in the tube and the bar, which are linearly dependent on each other. The characteristic loads distinguish this dependency to recognise a single load pattern which can be used to create both the cases (in tube and bar). In other words, if the assembly had n structural loadbearing elements instead of two (bar and tube), all the loading states of the system could still be represented in the characteristic load space of 2 dimensions (axial load and bending moment) instead of $2n$ dimensions. This is because the internal loads of the system will be a factor (dependent upon the stiffness of each element) of the two external loads.

1.4.5.1 Internal characteristic load from external characteristic load matrix

The above-discussed concepts can be applied at different levels and scales as well. The internal characteristic load matrix $L_{(N)_k}$ can be computed using the external characteristic load L_k^P. The internal load path for the two external characteristic $L_{(P)_k}$ is given by $N_{L_{(P)_k}}$ and is computed as in Eq. 0.17

$$N_{L_{(P)_k}} = L_{(P)_k}\,\Gamma \tag{0.17}$$

Now the matrix $N_{L_{(P)_k}}$ can be decomposed to identify the internal characteristic loads as Eq. 0.18

$$SVD(N_{L_{(P)_k}}) = U_{(N)_k} L_{(N)_k} \tag{0.18}$$

where $U_{(N)_k}$ and $L_{(N)_k}$ are the characteristic coefficient and characteristic load for the internal load matrix N respectively. Now the final internal load matrix is given as in Eq. 0.19

$$N_k = U_{(P)_k} U_{(N)_k} L_{(N)_k} \approx N \tag{0.19}$$

In conclusion, the characteristic loads reduce the original load cases to a smaller set by identifying the patterns in the original load case. In the example, the original internal load case set N of dimension (15×4) is effectively reduced to two characteristic loads $L_{(N)_k}$ of size (2×4) and a set of internal characteristic coefficients $U_{(N)_k}$.

1.5 Performance envelopes

The characteristic loads described above also serve another important purpose. By the property of the SVD decomposition, each row of the characteristic load matrix is orthonormal to every other row. Since the linear superposition of the characteristic loads recreates a load case (depending upon the characteristic coefficients), the characteristic loads can thus be used as the basis vectors of a new reduced space. This idea is the key enabler for the next topic of performance envelopes.

An interpretation of the characteristic load matrix is of a transformation matrix which maps loads from a higher dimensional *actual load space* (e.g. four dimensions of internal loads space) to a lower-dimensional *characteristic load space* (two dimensions).

The above idea of the characteristic load matrix being a transformation matrix can be used to map all loads acting on the structure to the characteristic load space. Therefore, it is also possible to find a combination of critical loads under which the structure fails. The region in the characteristic loads space wherein which the structure is safe is defined as the performance envelopes. The following section details the construction of a performance envelope for the compound bar assembly.

1.5.1 Failure modes of the compound bar assembly

The compound bar experiences failure when internal stress in the individual elements exceed the yield stress of the particular material, as given in Eq. 0.20.

$$\begin{aligned} \sigma_{tube}^{comp} &\leq \sigma_{tube}^{y=x1} \leq \sigma_{tube}^{tension} \\ \sigma_{bar}^{comp} &\leq \sigma_{bar}^{y=x3} \leq \sigma_{bar}^{tension} \\ \sigma_{tube}^{comp} &\leq \sigma_{tube}^{y=-x1} \leq \sigma_{tube}^{tension} \\ \sigma_{bar}^{comp} &\leq \sigma_{bar}^{y=-x3} \leq \sigma_{bar}^{tension} \end{aligned} \tag{0.20}$$

The assembly problem thus has eight different failure modes and the detailed calculation of the elemental stress $(\sigma_{tube}, \sigma_{bar})$ is presented in Appendix A. The superscript y refers to the maximum distance of the tube from the neutral axis. Since the bending moment is applied in

both directions (depending upon the load case), the compound bar assembly can fail either side of the neutral axis.

Eq. 0.20 can thus be represented as inequality constraints as given in Eq. 0.21.

$$\begin{bmatrix} \sigma_{tube}^{y=x1} \\ -\sigma_{tube}^{y=x1} \\ \sigma_{bar}^{y=x3} \\ -\sigma_{bar}^{y=x3} \\ \sigma_{tube}^{y=-x1} \\ -\sigma_{tube}^{y=-x1} \\ \sigma_{bar}^{y=-x3} \\ -\sigma_{bar}^{y=-x3} \end{bmatrix} \leq \begin{bmatrix} \sigma_{tube}^{ten} \\ \sigma_{tube}^{comp} \\ \sigma_{bar}^{ten} \\ \sigma_{bar}^{comp} \\ \sigma_{tube}^{ten} \\ \sigma_{tube}^{comp} \\ \sigma_{bar}^{ten} \\ \sigma_{bar}^{comp} \end{bmatrix} \tag{0.21}$$

The RF vector is given by Eq. 0.22

$$\boldsymbol{RF} = \begin{bmatrix} RF_1 \\ RF_2 \\ RF_3 \\ RF_4 \\ RF_5 \\ RF_6 \\ RF_7 \\ RF_8 \end{bmatrix} = \begin{bmatrix} RF_t^{ten} \\ RF_t^{com} \\ RF_b^{ten} \\ RF_b^{com} \\ RF_t^{ten,-y} \\ RF_t^{com,-y} \\ RF_b^{ten,-y} \\ RF_b^{com,-y} \end{bmatrix} \tag{0.22}$$

In the above Eq. 0.22, the individual RFs correspond to the eight failure modes. For example, RF_1 corresponds to the failure of the tube in tension. The superscript $-y$ represents the failure at the left-hand side of the neutral axis of the structure shown in Figure 0.1.

1.5.2 Identifying the performance envelope

Consider a point in a 2-dimensional characteristic load space given by $U_m = [U_1, U_2]$. This can be transformed to a point in internal load space N_m using Eq. 0.23.

$$N_m = U_m L_k \tag{0.23}$$

Using this for all failure modes (i.e. vector **RF**), it is now possible to map a set of load cases for which $RF = 1$ in characteristic load space, as shown in Figure 0.8.

The plot describes all the structural constraints of the assembly mapped on to the characteristic load space. Each line represents the combination of characteristic loads for which the corresponding RF is equal to one, i.e. the corresponding RF is about to be critical. For example, the solid red line describes the failure of the tube in tension at $y = +\frac{d}{2}$ whereas the dashed magenta represents the failure of the bar in compression at $y = -\frac{d}{2}$ and $d = 2x_1$

The region around the origin is marked by a black line, as shown in Figure 0.9, and this region represents the performance envelope of the structure. Any characteristic coefficient $U_m = [U_1, U_2]$ on the envelope is a combination of loads $(U_1L_1 + U_2L_2)$ for which $RF = 1$. Note that the constraints need to be convex to identify the performance envelope.

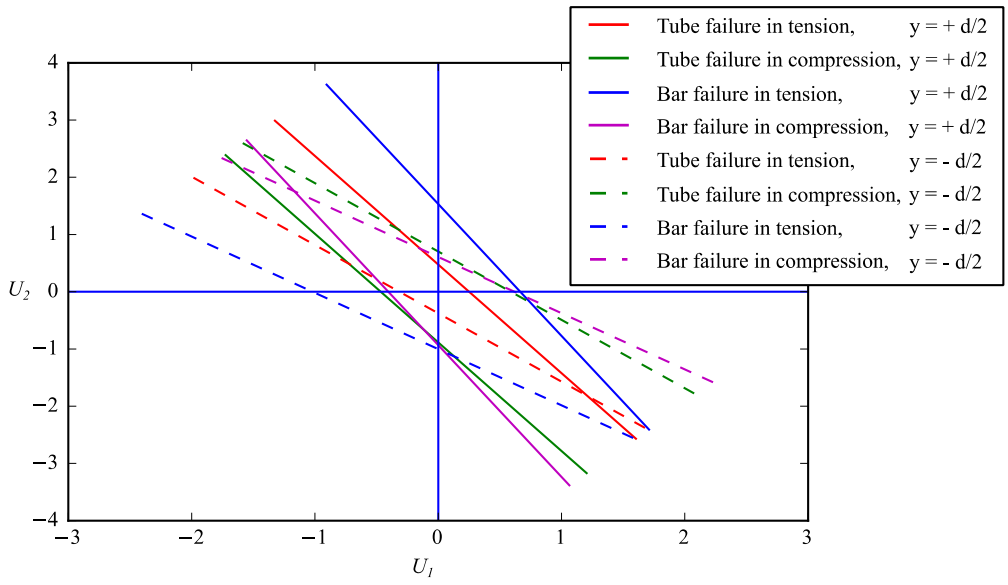

Figure 0.8: All eight failure modes of the compound bar assembly mapped into characteristic load space. The dotted lines represent a failure on the negative side of the neutral axis

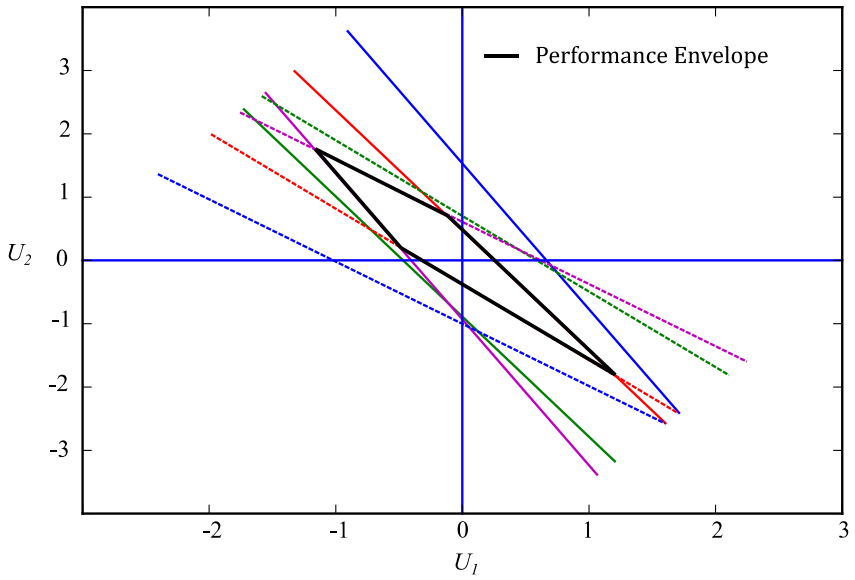

Figure 0.9: Performance envelope (in black) marked along with constraints in characteristic loads space

It is to be noted that the performance envelope identifies all the non-redundant constraints of the structure. For example, the green lines represent the failure of the tube in compression are not a part of the envelope and thus are never critical, i.e. the structure would have failed for a different failure mode before this failure ever becomes critical. Such constraints, if sufficiently far away from the envelope, can be ignored during structural sizing and optimisation. More discussion on this concept is presented in chapter 5.

From the above discussion, the performance envelope can be defined as a region around the origin of the characteristic loads space, which is bounded by all the non-redundant constraints. It essentially describes the load-bearing capacity of the structure.

1.5.3 Faceted approximation of envelopes

Complicated or unconventional structures may not have a direct analytical expression representing the failure of the system, unlike the compound bar assembly. In many industrial design cases, there may be a 'black box' approach to calculate failure which might include semi-empirical equations and rules such as the tools discussed in section **Error! Reference source not found.**

Building a performance envelope for such a problem will require a different technique. The original envelope can be approximated by using a number of facets, as shown in Figure 0.10.

The facets are identified using a point cloud based meshing routine in a spherical coordinate system.

This method involves two steps. The first step is a root finding step and solves for an equation to identify a point in the characteristic load space. The solved point results in a combination of characteristic loads that results in one of the reserve factors $RF = 1$.

The second step is a process to refine the mesh of the point cloud by adding points where they are needed to better define the critical surface of the performance envelope. This step decides the direction for which the root-finding needs to be carried out. The strategy of mesh refinement is presented in the subsequent section. Repeating the two steps results in a mesh of points in the characteristic load space and a convex hull [8] of these points will generate the required performance envelope. The convex hull for a set of points is defined as a convex closure that can contain all the points. An intuitive convex hull shape maybe visualised as a rubber band stretched around a set of nails on a board.

An iterative loop between the two steps is repeated until an appropriate number of points to approximate the actual performance envelope with a given fidelity. The fidelity of the approximate envelope is controlled by the mesh refinement algorithm, which is regulated by a defined RF tolerance ϵ_{RF}. A detailed discussion of both processes along with the novel improvements to the strategy is presented in **Error! Reference source not found.**.

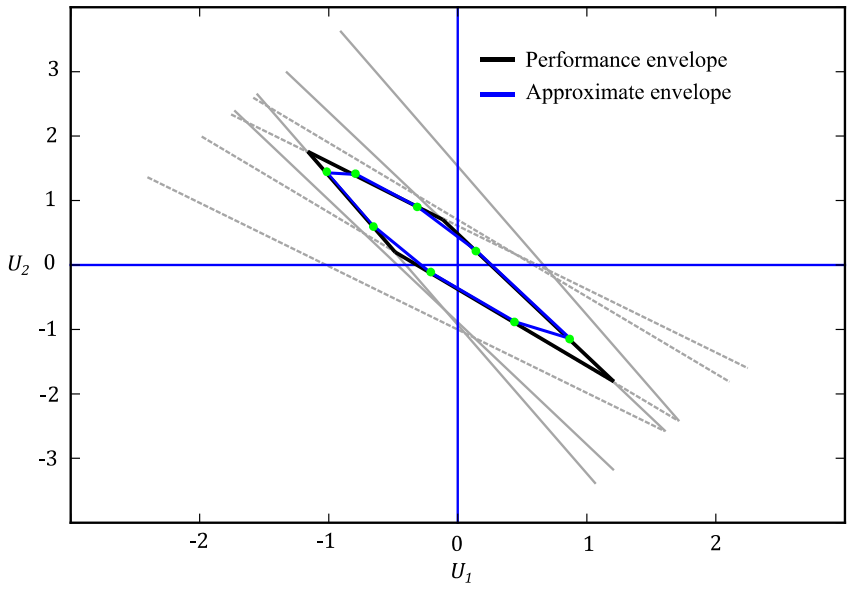

Figure 0.10: Performance envelope of the compound bar assembly in black along with a faceted approximate envelope in blue

1.6 Fast RF estimation

Fast Reserve Factor or Fast RF is a technique used to compute estimated RF values in a situation where the design is fixed but the load cases are updated [9]. This is typically the case in the period before aircraft certification when flight test measurements are used to make updates to the defined load cases. New RF values are based on the pre-certification RF results – essentially a performance envelope – and the updated load cases. In this thesis, the Fast RF is defined more generally as a technique to estimate the critical RF for a given load case from a performance envelope, and thereby enables the method to be used also for load case down selection at earlier design phases and for structural sensitivity computations, **Error! Reference source not found.**.

As defined in Eq. **Error! Reference source not found.**. the RF is the ratio of the allowable to the actual. In the characteristic loads space, the actual value of a load case is equal to the magnitude of the loads vector, and the allowable or the limiting value is equal to the intersection of the loads vector with the facet of the performance envelope as shown in Figure 0.11

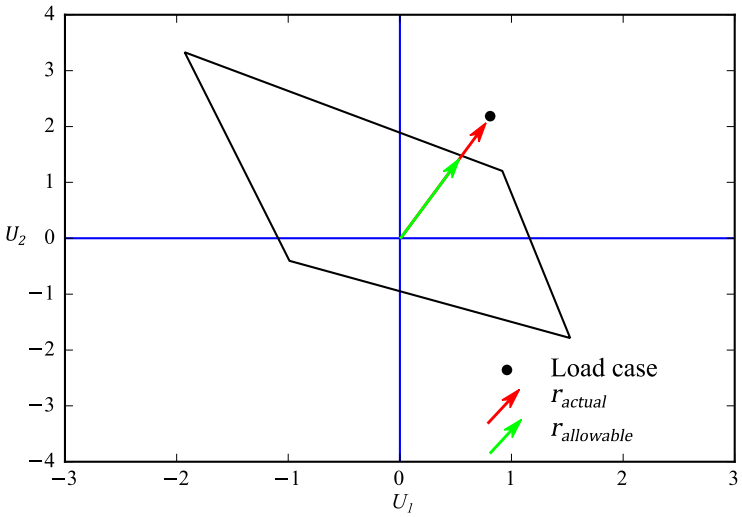

Figure 0.11: Fast RF method on a 2-dimensional performance envelope

The allowable magnitude in Eq. 0.24, $r_{allowable}$ for an arbitrary load case is calculated by a simple Ray-vector intersection.

$$RF = \frac{r_{allowable}}{r_{actual}} \tag{0.24}$$

For the set of 15 load cases, the RF are computed via the Fast RF method and are compared with a set of reference values. The reference values are obtained by solving the analytical constraints given in Eq. 0.22.

Figure 0.12 shows the scatter plot of the reciprocal of RF obtained from the Fast RF method to the analytical methods. The inverse of the RF is chosen because any load case of significant interest will have an RF close to or less than one. By taking the reciprocal, all the cases with large RF are grouped at the origin that can be ignored.

The results from the Fast RF estimated from the envelopes are in exceptionally good agreement with the reference values.

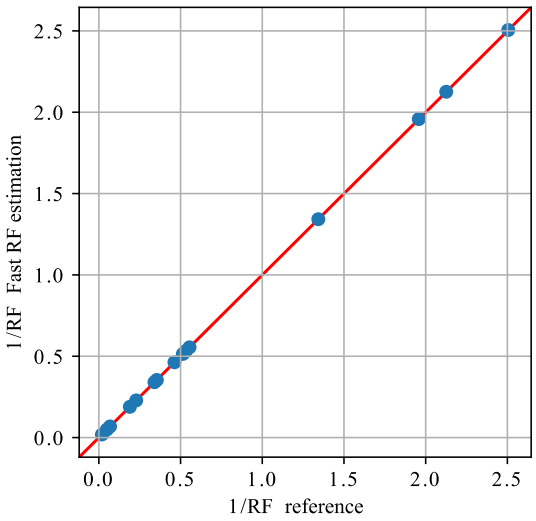

Figure 0.12: Scatter plot of inverse of RF, Fast RF vs reference values. Red line defines the line of equality

1.7 Summary

The chapter introduces a simple compound bar assembly problem. The assembly problem is used to give a generic explanation and demonstrate the concepts of characteristic loads, performance envelopes and Fast RF methods.

The four internal loads in the assembly are captured by two characteristic loads. These characteristic loads are used as basis vectors to define the characteristic loads space. The eight failure constraints of the assembly are mapped in the characteristic load space. This allows for the definition of performance envelopes. The method to approximately build performance envelope for a black box structural failure tool is discussed.

1.8 References

[1] A. Dharmasaroja, "Efficient modelling of failure envelopes and load patterns in aircraft structures," PhD PhD Thesis, School of Mechanical and Aerospace Engineering, Queen's University Belfast, Belfast, 2015.

[2] S. McGuinness, "Improving aircraft stress-loads interface and evaluation procedures," PhD Thesis, School of Mechanical and Aerospace Engineering, Queen's University Belfast, Belfast, 2011.

[3] MatWeb. "Aluminum 6061-O." http://www.matweb.com/search/DataSheet.aspx?MatGUID=626ec8cdca604f1994be4fc2bc6f7f63&ckck=1 (accessed 02/02/2020.

[4] MatWeb. "ASTM A36 Steel, bar." http://www.matweb.com/search/datasheet.aspx?matguid=d1844977c5c8440cb9a3a967f8909c3a&ckck=1 (accessed 02/02/2020.

[5] P. P. Benham, R. J. Crawford, and C. G. Armstrong, *Mechanics of Engineering Materials*. Longman Group, 1996.

[6] P. Virtanen *et al.*, "SciPy 1.0--Fundamental Algorithms for Scientific Computing in Python," *arXiv preprint arXiv:1907.10121*, 2019.

[7] A. Dharmasaroja *et al.*, "Load case characterization for the aircraft structural design process," *AIAA Journal*, pp. 2783-2792, 2017.

[8] C. B. Barber, D. P. Dobkin, D. P. Dobkin, and H. Huhdanpaa, "The quickhull algorithm for convex hulls," *ACM Transactions on Mathematical Software (TOMS)*, vol. 22, no. 4, pp. 469-483, 1996.

[9] J. Barron and F. Deru, "Fast Reserve Factor estimation," ed: Internal Airbus report RP1280239.